Wind and Structures, *Vol. 30, No. 4 (2020) 423-432*
DOI: https://doi.org/10.12989/was.2020.30.4.423

TMD effectiveness for steel high-rise building subjected to wind or earthquake including soil-structure interaction

Denise-Penelope N. Kontoni*[1] and Ahmed Abdelraheem Farghaly[2a]

[1]*Department of Civil Engineering, University of the Peloponnese, 1 M. Alexandrou Str., Koukouli, GR-26334 Patras, Greece*
[2]*Department of Civil and Architectural Constructions, Faculty of Industrial Education, Sohag University, Sohag 82524, Egypt*

(Received August 5, 2019, Revised October 25, 2019, Accepted October 26, 2019)

Abstract. A steel high-rise building (HRB) with 15 stories was analyzed under the dynamic load of wind or four different earthquakes taking into consideration the effect of soil-structure interaction (SSI) and using tuned mass damper (TMD) devices to resist these types of dynamic loads. The behavior of the steel HRB as a lightweight structure subjected to dynamic loads is critical especially for wind load with effect maximum at the top of the building and reduced until the base of the building, while on the contrary for seismic load with effect maximum at the base and reduced until the top of the building. The TMDs as a successful passive resistance method against the effect of wind or earthquakes is used to mitigate their effects on the steel high-rise building. Lateral displacements, top accelerations and straining actions were computed to judge the effectiveness of the TMDs on the response of the steel HRB subjected to wind or earthquakes.

Keywords: high-rise building (HRB); steel building; wind; earthquake; dynamic response; tuned mass damper (TMD); soil-structure interaction (SSI)

1. Introduction

Wind affects the buildings as a dynamic load because of is variation in the speed and of eddies and the value of dynamic effect on a HRB varies with the different parameters (such as the shape of the building, the surrounding, and the exposure angle of the wind). Earthquakes affect the buildings as dynamic loads and on a HRB as vibration effect because of the shaking of the soil under the foundation of the building. The TMD was checked over the past decades and has proven its effectiveness as a passive system to resist the dynamic impact of wind or earthquakes.

Kwon *et al*. (2008) illustrated the capabilities of NatHaz Aerodynamic Loads Database (NALD v. 2.0) in which users may select not only the data, but also may input desired power spectral density (PSD) expression or wind tunnel-derived PSD data set obtained from a HFBB experiment for the evaluation of wind load effects on high-rise buildings.

Zhou *et al*. (2008) studied the genetic algorithms (GA) and the Rayleigh damping optimum methods for wind-induced vibration control of a 20-storey high-rise steel building and adopted and 22 kinds of control plans to perform comparison analyses. Their results showed that the damping systems of MPD (mass proportional damping) and GAMPD (genetic algorithms and mass proportional damping) have the best performance of reducing structural wind-induced vibration response and are superior to other damping systems.

Gerasimidis *et al*. (2009) implemented a basic design optimization technique of tall steel structures for lateral loads, mainly wind, into trying to find the optimum locations and number of outriggers for a specific high-rise building; the structure is analyzed with all the possible outrigger locations monitoring important factors, such as the drift of the building or the moments on the core.

Chan *et al*. (2010) presented the analysis of equivalent static wind loads (ESWLs) on tall buildings with 3D modes provided that the wind tunnel derived aerodynamic wind load spectra are given and also developed an integrated wind load updating analysis and optimal stiffness design technique for lateral drift design of tall asymmetric buildings involving coupled lateral-torsional motions.

Pozos-Estrada *et al*. (2011) investigated the reliability of structures with tuned mass dampers under wind-induced motion and they showed that for structures that are designed or retrofitted without or with optimum linear TMDs and satisfying the same serviceability limit state criterion, their probability of exceeding the considered criterion is very consistent, however this consistency deteriorates if nonlinear TMDs are employed.

Heiza and Tayel (2012) compared the effects of wind and earthquake loads on reinforced concrete high-rise buildings and concluded that wind is more effective than earthquake for tall buildings with shear walls when minimum design factors are considered, earthquake is more effective for short buildings, while the wind and earthquake effects increase rapidly when the height of the building increases.

Cluni *et al*. (2013) proposed two reduced-order

*Corresponding author, Associate Professor
E-mail: kontoni@teiwest.gr, kontoni@uop.gr
[a]Associate Professor
E-mail: farghaly@techedu.sohag.edu.eg

ISSN: 1226-6116 (Print), 1598-6225 (Online)

equivalent shear-beam models in order to estimate the dynamic response of tall buildings affected by wind loads.

Aly (2013) presented a pressure integration technique for response prediction in high-rise buildings under wind loads and this proposed procedure has the advantages of accounting for complex mode shapes, non-uniform mass distribution, and interference effects from the surrounding and also the contribution of higher modes.

Yi *et al*. (2013) investigated the dynamic characteristics and wind-induced vibrations of a 420 m high building during typhoons by using accelerometers and GPS mounted in the building. The multipath effects are extracted by a combination of Empirical Mode Decomposition and wavelet method, and then are removed by a high pass Finite Impulsive Response digital filter to improve the performance of the GPS.

Zhang *et al*. (2014) conducted an experimental investigation to quantify the characteristics of the microburst-induced wind loads (i.e., both static and dynamic wind loads) acting on a high-rise building model, compared to those with the test model placed in conventional atmospheric boundary layer (ABL) winds and it was found that the microburst-induced wind loads acting on high-rise buildings would be significantly different from their counterparts in conventional ABL winds.

Huang *et al*. (2014) studied the characteristics of amplitudes and power spectra of X, Y and RZ axial wind forces on a 492 m high-rise building with section varying along the height and proposed the corresponding mathematical expressions of power spectra of X axial (across-wind), Y axial (along-wind) and torsional wind forces.

Huang *et al*. (2015) studied the characteristics of the coherence functions of X axial, Y axial, and RZ axial wind forces on a 492 m high-rise building with section varying along height via a synchronous multi-pressure measurement of the rigid model in wind tunnel simulating of the turbulent and proposed the corresponding mathematical expressions of the coherence functions.

Aly *et al*. (2015) studied the application of hybrid tuned mass and magneto-rheological (TM/MR) dampers for the control of wind-induced motion in high-rise buildings and by a dissipative analysis showed that the MR dampers are working within the possible range of optimum performance.

Ross *et al*. (2015) studied a real high-rise building to show the effectiveness and robustness of the tuned liquid dampers (TLDs) in reducing the coupled lateral-torsional motion of this high-rise building under wind load. Three multi-modal TLD systems are designed to mitigate the torsional response of the building and three practical parameters are varied to investigate the robustness of the TLD system: the height of the water inside the tanks, the amplitude modification factor and the structural modal frequencies.

Farouk (2016) applied computational fluid dynamics (CFD) to check the comfort of the occupants at a high-rise in Norway and found good agreement in their numerical model results with those of others obtained using codes.

Giaralis and Petrini (2017) coupled the classical linear tuned mass damper (TMD) with an inerter in various tuned mass-damper-inerter (TMDI) topologies to suppress excessive wind-induced oscillations in tall buildings and they concluded that the TMDI reduces peak top-floor acceleration more effectively than the TMD that the TMDI meets code-prescribed serviceability design requirements for new tall buildings while it can also be used to upgrade the performance of existing TMD-equipped tall buildings without changing the attached mass.

Farghaly and Kontoni (2018) by developing a realistic FEM nonlinear structural model, predicted the behavior, load transfer, force distribution and performance of a riverine platform under earthquake and environmental loads (wind, wave and current loads).

Pozos-Estrada (2018) developed an empirical expression that includes the uncertainties in wind-climate, structural properties, perception of motion and maximum response, and incorporated them into a simple procedure to evaluate the wind-induced acceleration in tall buildings.

Huang *et al*. (2018) performed 3D simulations based on an impinging jet to investigate the flow field of a steady downburst and its effects on a high-rise building by applying the SST k-w turbulence model. The flow around the building, pressure distributions on the building surfaces and aerodynamic forces were analyzed in order to enhance the understanding of wind load characteristics on a high-rise building immersed in a downburst.

Wind and earthquake behave as natural destructive forces affecting the HRB in the same way as a lateral force, but the wind loads act from the top of the building until the foundation level with varying load values and the earthquake affects the building from the foundation level as a shaking reversible force. The effects of wind and earthquake loads have the ability to destroy the buildings, especially if these dynamic loads are not taken into consideration in the design. A steel HRB with 15 stories was checked for its behavior under wind or four different earthquakes taking into consideration the effect of soil-structure interaction (SSI) and using tuned mass dampers (TMDs) to resist these types of dynamic loads as a passive way and to show which dynamic load can be better resisted by the TMDs.

2. Model description including SSI

The model studied is a steel HRB of 15 storeys (each floor's height 3 m) as shown in Fig. 1 with two foundation cases: the first is fixed base and the second is raft foundation including SSI.

The beams and columns are represented in SAP2000 as frame elements with columns cross-section constant all over the height of the model; the columns are B.F.I.B. No. 50 and the beams' cross-sections are S.I.B. No. 30, all connections are welded. The slabs and the raft foundation elements are represented in SAP2000 as shell elements. Fig. 1(a) shows the structural plan of the typical floor of the model, Fig. 1(b) represents the raft foundation system for the model with thickness equals to 2000 mm and upper and lower mesh reinforcements 7#22/m. Fig. 1(c) shows the top floor of the model having four TMD devices. The

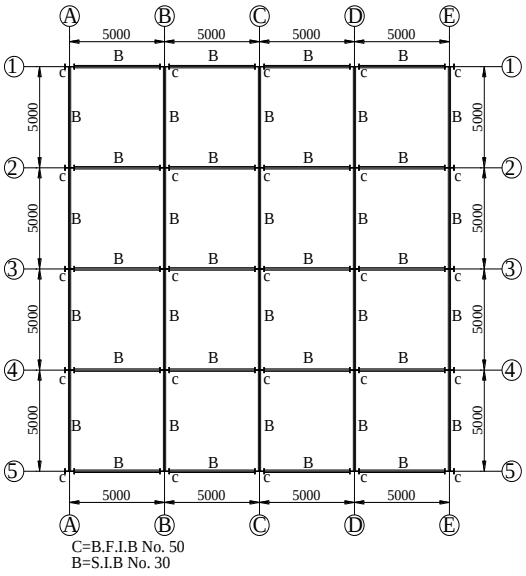

(a) Typical structural plan (mm)

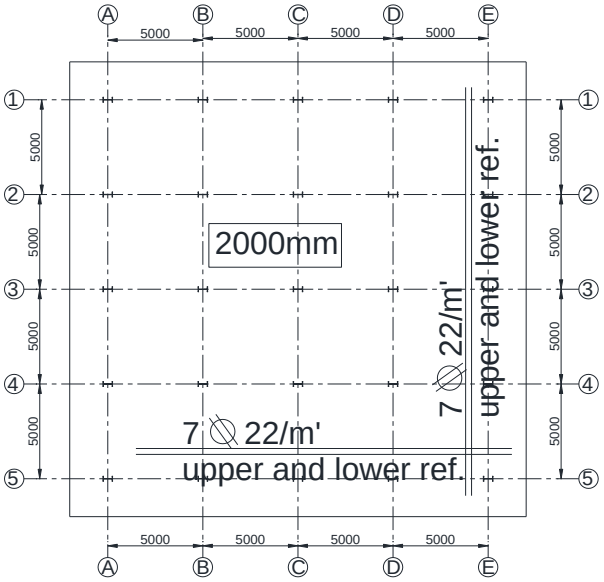

(b) Raft foundation system (mm)

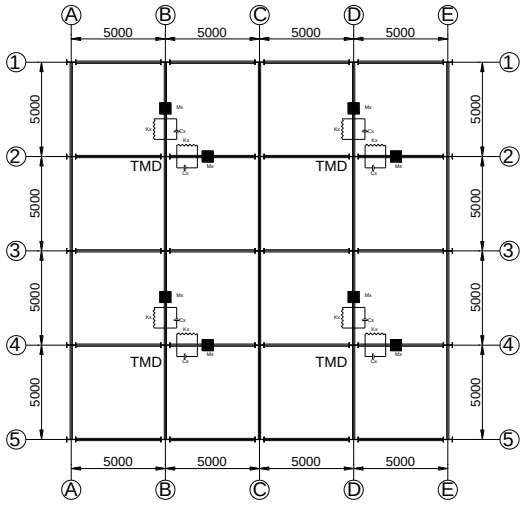

(c) Plan of the top floor of the model (mm)

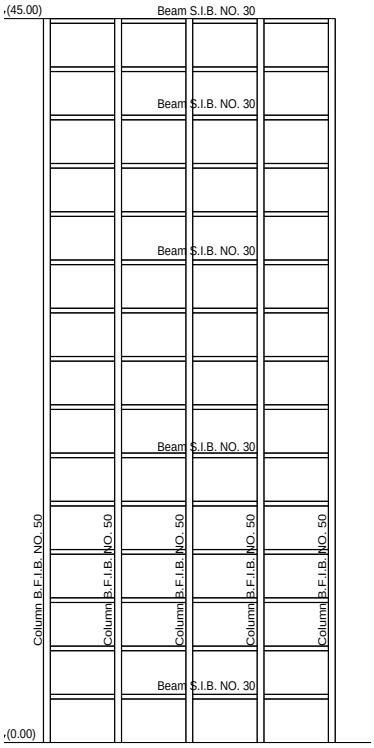

(d) Elevation

Fig. 1 Model of the steel HRB

specifications of the installed TMDs and the optimum values of the TMD parameters are as in Farghaly (2017). Fig. 1(d) shows the elevation of the model with 15 storeys.

The soil under the raft foundation is represented by 3D elements, as described by Farghaly and Ahmed (2013) and Fig. 2 shows these SSI elements which are used as soil elements under the raft foundation.

The dead load was computed by the SAP2000 and the live load on the slabs was taken as 2 KN/m^2. The dynamic loads which the model was subjected to were four different bidirectional earthquakes (El Centro, Chi-Chi, Loma Prieta, Hollister earthquakes as shown in Figs. 3(a) - 3(d), and wind loads in both directions x, y of the model (as shown in Fig. 4).

The time history analysis was used in the analysis of all the steel HRB model cases.

3. Seismic loads

The steel HRB model was subjected to four different earthquakes equal in x and y directions. These earthquakes

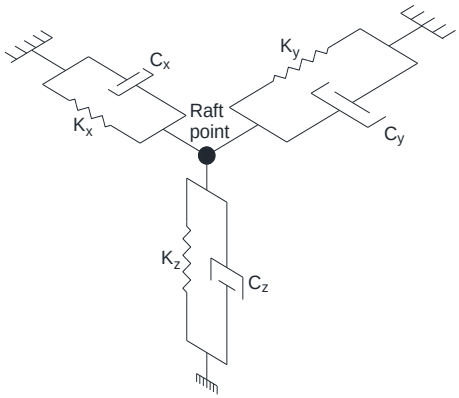

Fig. 2 Three-dimensional elements representing the soil under the raft foundation

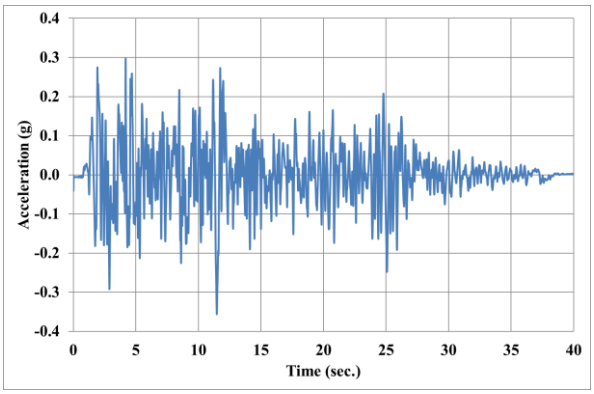

(a) El Centro

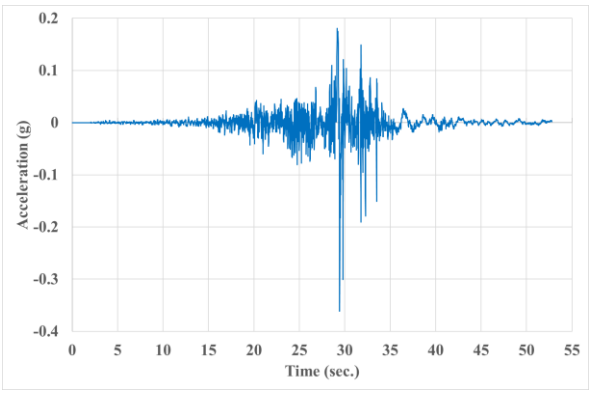

(b) Chi-Chi

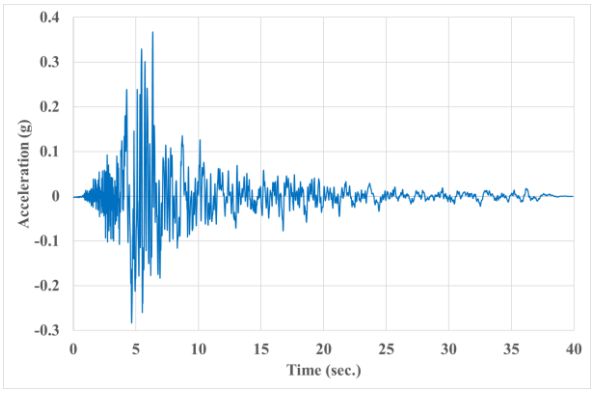

(c) Loma Prieta

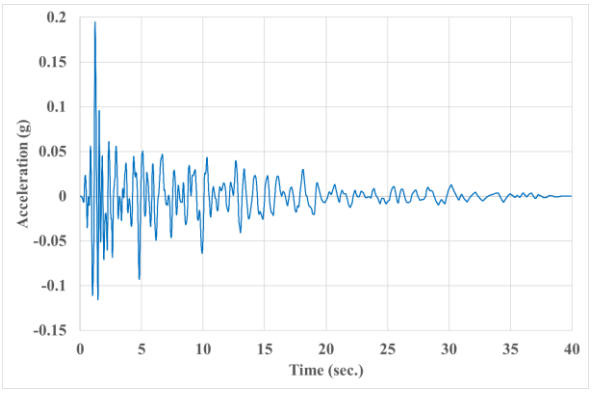

(d) Hollister

Fig. 3 Earthquake accelerograms

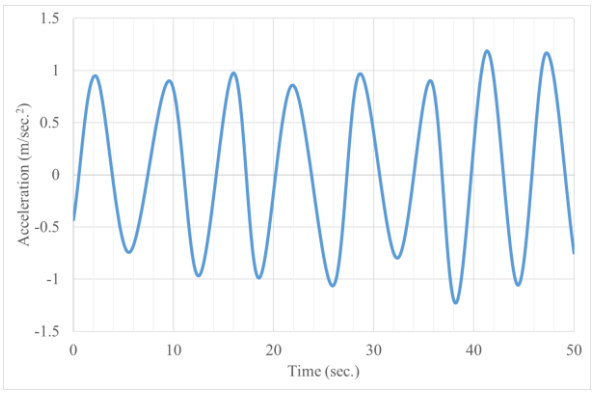

(a) Along-wind direction

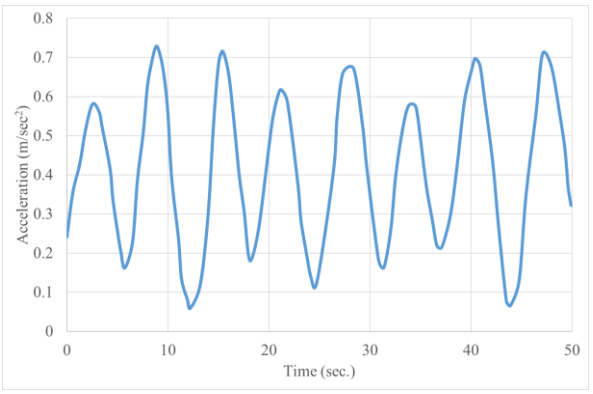

(b) Across-wind direction

Fig. 4 Wind acceleration in both directions x and y, as a result of wind blow perpendicular to the model

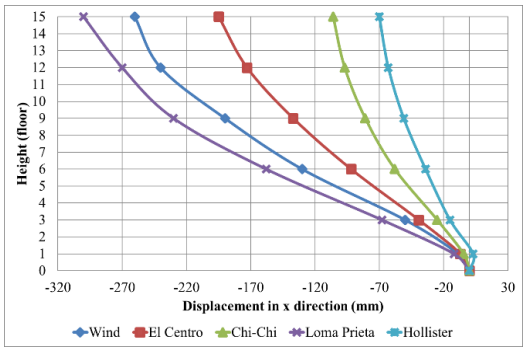

(a)

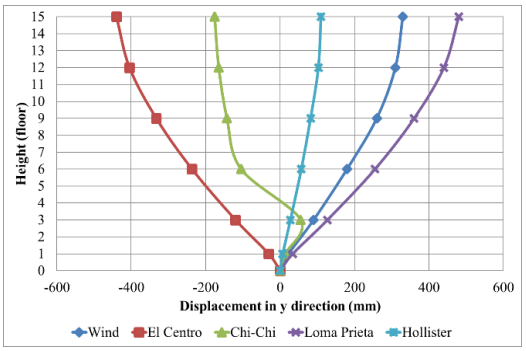

(b)

Fig. 5 Displacements in x and y directions for fixed base case

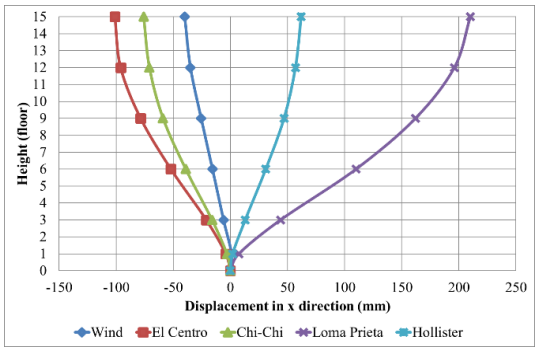

(a)

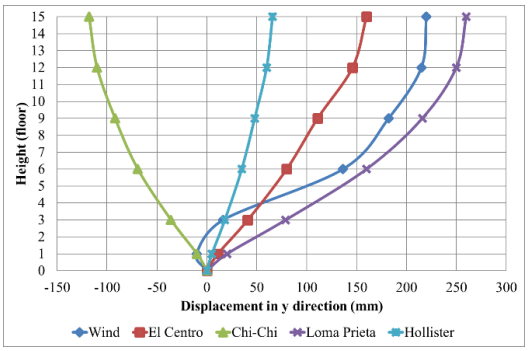

(b)

Fig. 6 Displacements in x and y directions for fixed base and TMDs on the top of the model

were the 1940 El Centro earthquake that occurred in California with magnitude 6.9, the 1999 Chi-Chi earthquake that occurred in Taiwan with magnitude 7.6, the 1989 Loma Prieta earthquake that occurred in Northern California with magnitude of 6.9, and the Hollister earthquake that occurred near central California with magnitude 5.2, as shown in Figs. 3(a) - 3(d).

4. Wind loads

In order to show the dynamic effect of the wind on the steel HRB using SAP2000 the dynamic effect will be applied on the joints of the model gradually with the highest values in the top of the model and then decreasing with decreasing the height of the model.

The wind loads which the model is subjected to as a result of wind blow perpendicular to the model (Persson *et al*. 2016) are wind accelerations (as shown in Fig. 4) in both directions x and y (i.e., along and across wind direction) with time duration of the wind effect 50 seconds. Fig. 4(a) shows the acceleration of the wind in the along-wind direction and Fig. 4(b) shows the acceleration of the wind in the across-wind direction.

5. Results and discussion

The effects of the wind and earthquakes on the steel HRB with SSI were considered to show the effectiveness of TMDs on the resistance of these dynamic loads including SSI as a realistic model; the steel HRB was selected as a lightweight construction with a damping coefficient equal to 0.02 (which is less than the reinforced concrete damping coefficient 0.05). Four TMDs were installed on the roof of the model distributed 10m apart, while each TMD is bidirectional in x and y directions to resist in both directions.

The response of the steel HRB is different in x and y directions because of the direction of the web of the cross-section of the steel columns; the directions of the web of steel columns are in x direction.

Figs. 5 - 8 shows the displacements in the x and y directions for the steel HRB model for different cases, namely fixed or raft foundation cases, with or without TMDs, under wind or different earthquakes, in order to show the effectiveness of the TMDs in resisting the dynamic effect of wind or earthquakes.

Fig. 5(a) shows the displacements in x direction of each floor for the fixed base case; the highest lateral displacements were recorded for the Loma Prieta earthquake while the lowest lateral displacements for the Hollister earthquake; the nearest lateral displacements for the Loma Prieta earthquake were the wind case; all the displacements are in one direction. Fig. 5(b) shows the lateral displacements in y direction; all values are higher than the lateral displacements in x direction (the directions of the web of steel columns are in x direction) while the

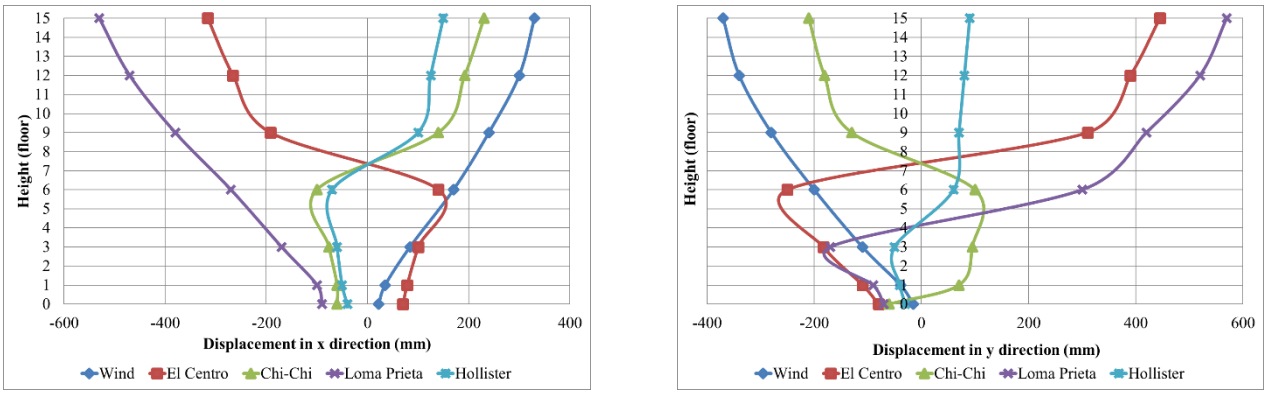

(a) (b)

Fig. 7 Displacements in x and y directions with SSI effect

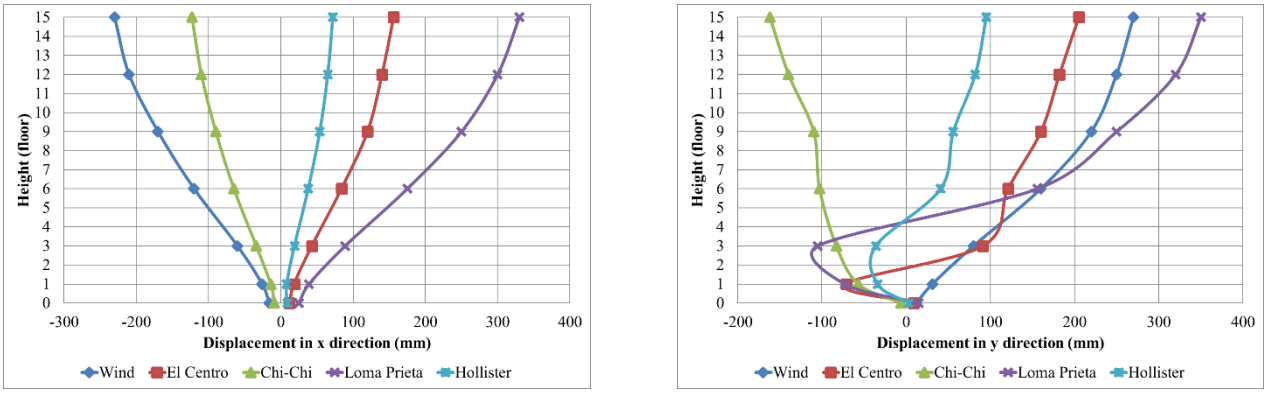

(a) (b)

Fig. 8 Displacements in x and y directions with SSI and TMDs on the top of the model

maximum lateral displacements record for the Loma Prieta earthquake and the wind case has the nearest values to it.

Figs. 6(a) and 6(b) show the lateral displacements in x and y directions of the fixed base model with TMDs installed on its top; in the x direction the lateral displacements decrease by nearly 50% for the El Centro earthquakes, by nearly 30% for the Loma Prieta, while for the Hollister and Chi-Chi earthquakes the TMDs nearly did not affect the values of the lateral displacements but for the wind load case the lateral displacements decreased by 540% than the case without TMDs. The TMDs decreased the lateral displacements in the y direction for the Loma Prieta, Hollister, El Centro and Chi-Chi earthquakes by nearly 50% but for the wind load case the TMDs decreased displacements by nearly 145%.

Figs. 7(a) and 7(b) represent the lateral displacements in x and y directions for the model with SSI effect under different earthquakes or wind load in addition to the live and dead loads acting on the model. Fig. 7(a) shows the lateral displacements of the model in x direction; the maximum displacement values appear in the Loma Prieta earthquake, while in the other earthquake records displacements have smaller values, and the wind load case records medium lateral displacement values. Fig. 7(b) represents the y direction lateral displacements which the values nearly like the corresponding values in x direction lateral displacements but with different displacement signs.

Figs. 8(a) and 8(b) show the lateral displacements in x and y directions for the model with SSI effect and installed TMDs on the top of the model subjected to earthquakes or wind. Fig. 8(a) represents the lateral displacements in x direction with SSI effect and TMDs installed on the top of the model; wind load case nearly is not affected, while in earthquake cases the lateral displacements in x direction reduce by nearly 50% for all kinds of earthquakes except for Loma Prieta earthquake where TMDs reduced the lateral displacement by nearly 57% than the case without TMDs. Fig. 8(b) shows the lateral displacements in y direction with SSI and TMDs installed on the top of the model; for wind load case the TMDs nearly did not affect the lateral displacements, for Loma Prieta earthquake the TMDs reduced the lateral displacements by nearly 71%, while the rest cases of earthquakes nearly are not affected by installing TMDs.

Fig. 9 shows the top accelerations of the model under wind or earthquake loads, with the effect of SSI and TMDs or without. Fig. 9(a) represents the top accelerations in x direction of the model; the accelerations increased especially in the fixed base case and TMDs fixed base case, but they decreased sharply when the SSI effect was taken into consideration where the effect of TMDs with SSI is not considerable. Fig. 9(b) represents the top accelerations of the model in y direction which are nearly close to the x direction accelerations but in case of TMDs with fixed base

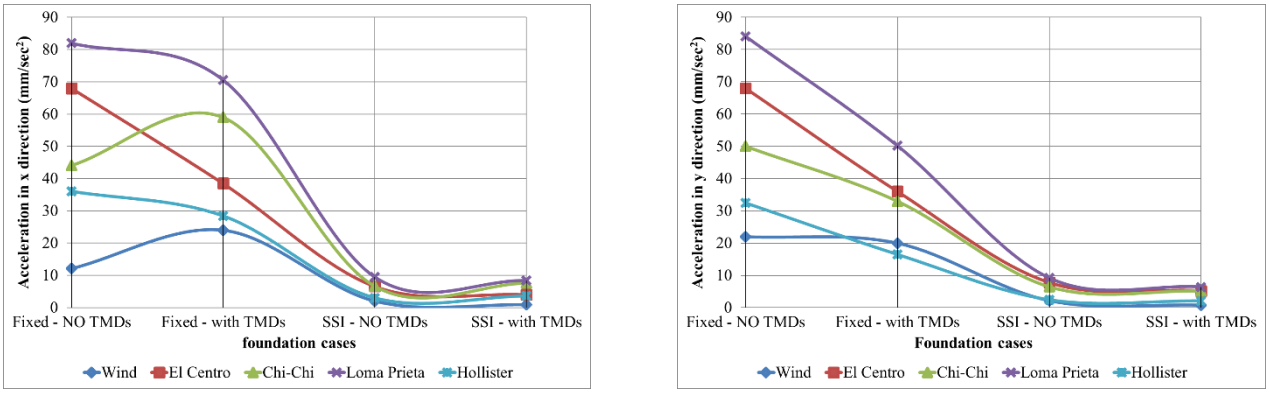

(a) (b)

Fig. 9 Top accelerations in x and y directions

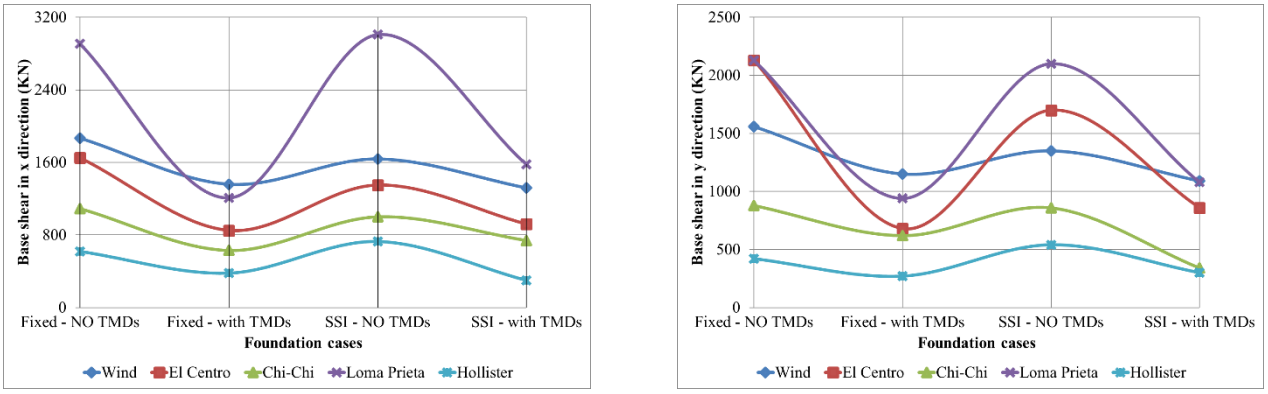

(a) (b)

Fig. 10 Base shear forces in x and y directions

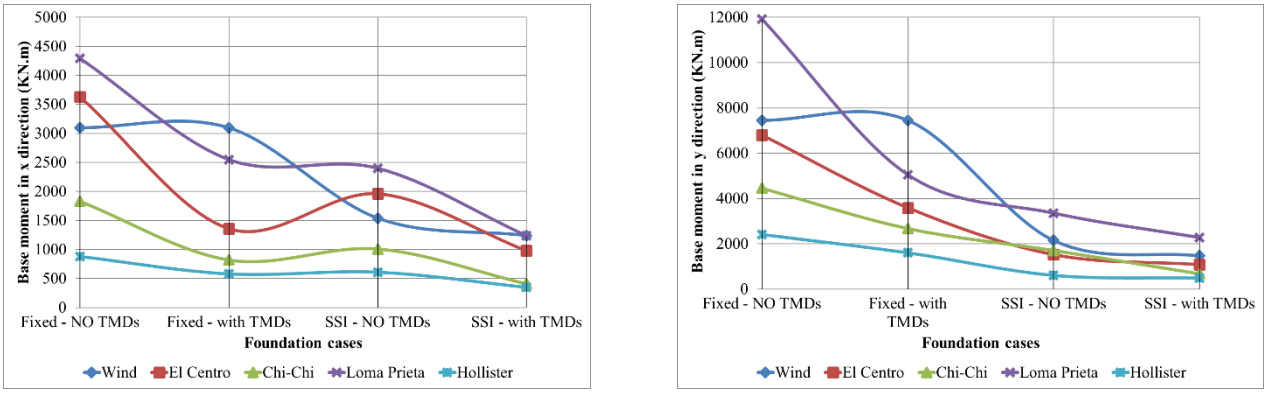

(a) (b)

Fig. 11 Base bending moments in x and y directions

reduced than the fixed base case by nearly 1.7 times for all load cases, and again the use of TMDs with SSI is not considerable.

Fig. 10 shows the base shear forces of the model under different loads. Fig. 10(a) shows the base shear of the model in x direction; the effects of TMDs with SSI and TMDs with fixed base are nearly equal, the effect of TMDs is nearly not considerable except for the Loma Prieta earthquake where the effect of TMDs with SSI reduces the base shear by nearly 50%. Fig. 10(b) shows the base shear in y direction of the model; the effect of TMDs with SSI reduces the base shear in the wind load case by nearly 40% than with SSI without TMDs, also in the Chi-Chi, El Centro and Loma Prieta earthquakes the TMDs with SSI reduce the base shear forces in y direction by nearly 46% than SSI effect without TMDs.

Fig. 11 represents the base moments of the model under different loads. Fig. 11(a) shows base moments in x direction; wind loads base moment reduced by nearly 25% than without TMDs, Loma Prieta base moment reduced by 1.67 times than without TMDs, El Centro and Chi-Chi reduced by 50%, the fixed base shows the same trend of the

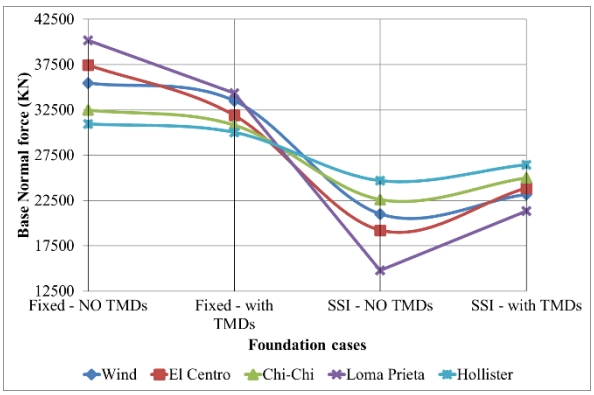

Fig. 12 Base normal forces

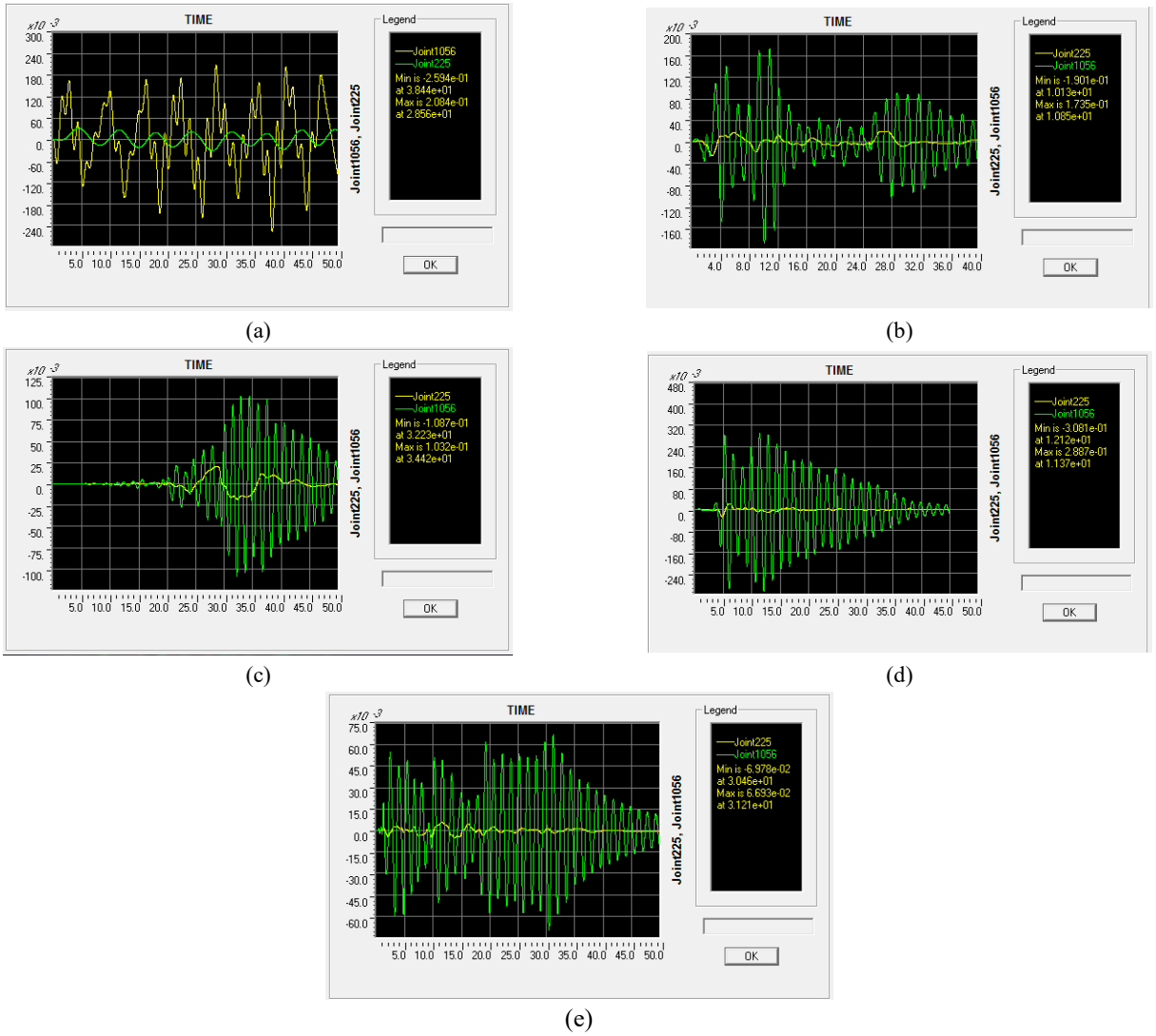

Fig. 13 Lateral top displacements for the fixed base HRB model with TMDs ("Joint 225") and without TMDs ("Joint 1056")

effect of TMDs in reduction base moment. Fig. 11(b) shows the base moment in y direction, base moment reduce by nearly 40% in TMDs with SSI than SSI without TMD in Loma Prieta earthquake and in wind, reduced by nearly 10% and in El Centro, Chi-Chi, and Hollister reduce by nearly 8%, the fixed base with TMDs reduced the base moment than fixed base without TMDs in Earthquakes El Centro and Chi-Chi by nearly 1.75 times but nearly not affect in wind and Hollister loads.

Fig. 12 represents base normal force in the model the effect of TMDs with SSI for Hollister and Chi-Chi and wind are nearly not affected but base normal force increased by nearly 1.50 times than SSI without TMDs for Loma Prieta and El Centro earthquakes but for wind and Chi-Chi

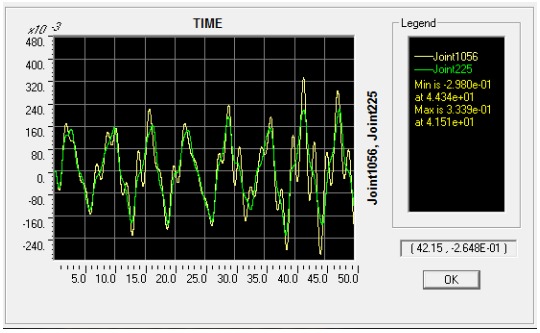

(a) Wind (SSI)

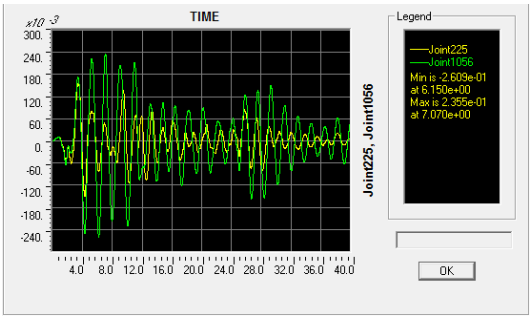

(b) El Centro (SSI)

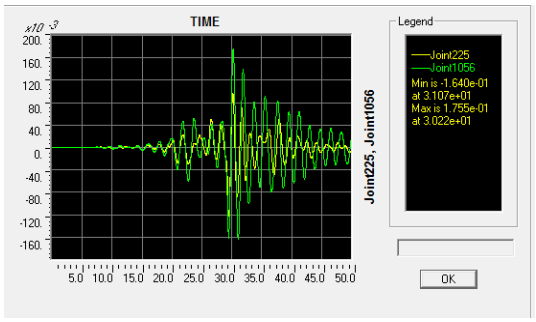

(c) Chi-Chi (SSI)

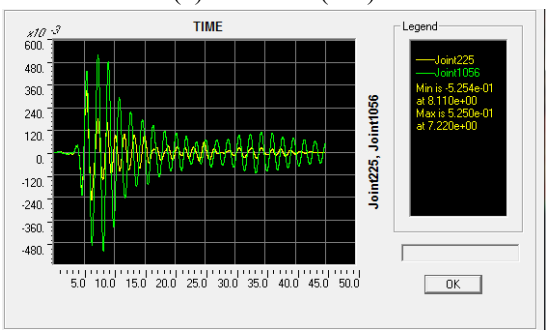

(d) Loma Prieta (SSI)

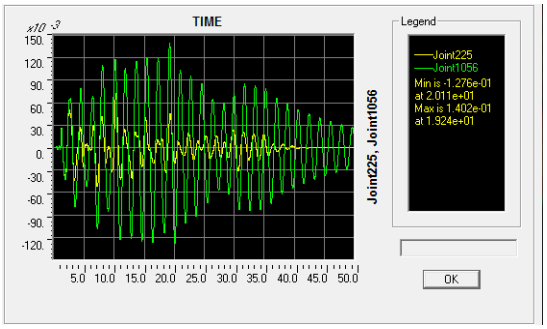

(e) Hollister (SSI)

Fig. 14 Lateral top displacements for the HRB SSI model with TMDs ("Joint 225") and without TMDs ("Joint 1056")

increased by 12% than without TMDs, the same trend repeated in the fixed base case.

Fig. 13 illustrates the comparison of vibration of the lateral top point displacement of the HRB model with fixed base under different dynamic load cases (wind or earthquakes) using TMDs and without using TMDs and the reduction effect of the TMDs on the lateral displacements is clearly shown

Fig. 14 illustrates the comparison of vibration of the lateral top point displacement of the HRB model taking into consideration the SSI effect under different dynamic load cases (wind or earthquakes) using TMDs and without using TMDs and the reduction effect of the TMDs on the lateral displacements is shown.

6. Conclusions

A steel HRB with 15 stories was analyzed under the dynamic load of wind or earthquakes. The behavior of the steel HRB as a lightweight structure subjected to dynamic loads is critical especially for wind load with effect maximum at the top of the building and reduced until the base of the building, while on the contrary for seismic load with effect maximum at the base and reduced until the top of the building. The TMDs as a successful passive resistance method against the effect of wind or earthquakes is used to mitigate their effects on the steel high-rise building. Lateral displacements, top accelerations and straining actions were computed to judge the effectiveness of the TMDs on the response of the steel HRB subjected to wind or earthquakes and from the calculated results, the following conclusions can be drawn out:

- The response of the steel HRB is different in x and y directions because of the direction of the web of the cross-section of the steel columns (the difference between x and y directions may be reached to 2 times).
- The lightness of a steel HRB is considered a great challenge in resisting wind loads.
- The TMDs affects the straining actions of the model with fixed base more than the corresponding values in the model with SSI.
- The reduction effect on the earthquake loads is greater than on the wind load when using TMDs.

References

Aly, A.M. (2013), "Pressure integration technique for predicting wind-induced response in high-rise buildings", *Alexandria Eng. J.*, **52**, 717-731. http://dx.doi.org/10.1016/j.aej.2013.08.006.

Aly, A.M. (2015), "Control of wind-induced motion in high-rise buildings with hybrid TM/MR dampers", *Wind Struct.*, **21**(5), 565-595. http://dx.doi.org/10.12989/was.2015.21.5.565.

Chan, C.M., Huang, M.F. and Kwok, K.C.S. (2010), "Integrated wind load analysis and stiffness optimization of tall buildings with 3D modes", *Eng. Struct.*, **32**(5), 252-1261. http://dx.doi.org/10.1016/j.engstruct.2010.01.001.

Cluni, F., Gioffrè, M. and Gusella, V. (2013), "Dynamic response of tall buildings to wind loads by reduced order equivalent shear-beam models", *J. Wind Eng. Ind. Aerod.*, **123**, 339-348. https://doi.org/10.1016/j.jweia.2013.09.012.

Farghaly, A.A. and Ahmed, H.H. (2013), "Contribution of soil-structure interaction to seismic response of buildings", *KSCE J. Civil Eng.*, **17**(5), 959-971. https://doi.org/10.1007/s12205-013-0261-9.

Farghaly, A.A. (2017), "Self-control of high rise building L-shape in plan considering soil structure interaction", *Coup. Syst. Mech.*, **6**(3), 229-249. https://doi.org/10.12989/csm.2017.6.3.229.

Farghaly, A.A. and Kontoni, D.P.N. (2018), "Nonlinear analysis of a riverine platform under earthquake and environmental loads", *Wind Struct.*, **26**(6), 343-354. https://doi.org/10.12989/was.2018.26.6.343.

Farouk, M.I. (2016), "Check the comfort of occupants in high rise building using CFD", *Ain Shams Eng. J.*, **7**(3), 953-958. https://doi.org/10.1016/j.asej.2015.06.011.

Gerasimidis, S., Efthymiou, E. and Baniotopoulos, C.C. (2009), "Optimum outrigger locations of high-rise steel buildings for wind loading", *EACWE Florence*, 1-10. http://www.iawe.org/Proceedings/5EACWE/029.pdf.

Giaralis, A. and Petrini, F. (2017), "Wind-induced vibration mitigation in tall buildings using the tuned mass-damper-inerter", *J. Struct. Eng.*, **143**(9), 04017127. https://doi.org/10.1061/(ASCE)ST.1943-541X.0001863.

Heiza, K.M. and Tayel, M.A. (2012), "Comparative study of the effects of wind and earthquake loads on high-rise buildings", *Concrete Res. Let.*, **3**(1), 386-405. http://www.issres.net/journal/index.php/crl/article/view/257/150.

Kwon, D.K., Kijewski-Correa, T. and Kareem, A. (2008), "e-Analysis of high-rise buildings subjected to wind loads", *J. Struct. Eng.*, **134**(7), 1139-1153. https://doi.org/10.1061/(ASCE)0733-9445(2008)134:7(1139).

Huang, D.M., Zhu, L.D. and Chen, W. (2014), "Power spectra of wind forces on a high-rise building with section varying along height", *Wind Struct.*, **18**(3), 295-320. http://dx.doi.org/10.12989/was.2014.18.3.295.

Huang, D.M., Zhu, L.D., Chen, W. and Ding, Q.S. (2015), "Vertical coherence functions of wind forces and influences on wind-induced responses of a high-rise building with section varying along height", *Wind Struct.*, **21**(2), 119-158. http://dx.doi.org/10.12989/was.2015.21.2.119.

Huang, G., Liu, W., Zhou, Q., Yan, Z. and Zuo, D. (2018), "Numerical study for downburst wind and its load on high-rise building", *Wind Struct.*, **27**(2), 89-100. http://dx.doi.org/10.12989/was.2018.27.2.089.

Persson, P., Austrell, P.E., Kirkegaard, P.H., Andersen, L.V. and Steffen, F. (2016), "Analysis of wind-induced vibrations in high-rise buildings", *Proceedings of the 45th International Congress and Exposition on Noise Control Engineering: Towards a Quieter Future*, Germany, August.

Pozos-Estrada, A., Hong, H.P. and Galsworthy, J.K. (2011), "Reliability of structures with tuned mass dampers under wind-induced motion: a serviceability consideration", *Wind Struct.*, **14**(2), 113-131. http://dx.doi.org/10.12989/was.2011.14.2.113.

Pozos-Estrada, A. (2018), "A simple procedure to evaluate the wind-induced acceleration in tall buildings: An application to Mexico", *Wind Struct.*, **27**(5), 337-445. http://dx.doi.org/10.12989/was.2018.27.5.337.

Ross, A.S., El Damatty, A.A. and El Ansary, A.M. (2015), "Application of tuned liquid dampers in controlling the torsional vibration of high rise buildings", *Wind Struct.*, **21**(5), 537-564. http://dx.doi.org/10.12989/was.2015.21.5.537.

SAP2000® Version 17 (2015), Integrated Software for Structural Analysis and Design; Computers and Structures, Inc., Walnut Creek, CA and New York, U.S.A. https://www.csiamerica.com/products/sap2000.

Yi, J., Zhang, J.W. and Li, Q.S. (2013), "Dynamic characteristics and wind-induced responses of a super-tall building during typhoons", *J. Wind Eng. Ind. Aerod.*, **121**, 116-130. https://doi.org/10.1016/j.jweia.2013.08.006.

Zhang, Y., Sarkar, P. and Hu, H. (2014), "An experimental study on wind loads acting on a high-rise building model induced by microburst-like winds", *J. Flu. Struct.*, **50**, 547-564. https://doi.org/10.1016/j.jfluidstructs.2014.07.010.

Zhou, Y. Wang, D.Y. and Deng, X.S. (2008), "Optimum study on wind-induced vibration control of high-rise buildings with viscous dampers", *Wind Struct.*, **11**(6), 497-512. http://dx.doi.org/10.12989/was.2008.11.6.497.

CC